

## OPEN ACCESS

## EDITED BY

Mirjam Schenk,  
University of Bern, Switzerland

## REVIEWED BY

Jennifer L. Larson-Casey,  
University of Alabama at Birmingham,  
United States  
Jae-Hyuk Yu,  
University of Wisconsin-Madison,  
United States

## \*CORRESPONDENCE

Do-Young Yoon  
✉ ydy4218@konkuk.ac.kr

<sup>†</sup>These authors contributed equally to  
this work

RECEIVED 07 February 2023

ACCEPTED 26 April 2023

PUBLISHED 09 May 2023

## CITATION

Park J-Y, Park H-M, Kim S, Jeon K-B,  
Lim C-M, Hong JT and Yoon D-Y (2023)  
Human IL-320A94V mutant attenuates  
monocyte-endothelial adhesion by  
suppressing the expression of ICAM-1 and  
VCAM-1 via binding to cell surface  
receptor integrin  $\alpha V\beta 3$  and  $\alpha V\beta 6$  in TNF- $\alpha$ -  
stimulated HUVECs.  
*Front. Immunol.* 14:1160301.  
doi: 10.3389/fimmu.2023.1160301

## COPYRIGHT

© 2023 Park, Park, Kim, Jeon, Lim, Hong and  
Yoon. This is an open-access article  
distributed under the terms of the [Creative  
Commons Attribution License \(CC BY\)](#). The  
use, distribution or reproduction in other  
forums is permitted, provided the original  
author(s) and the copyright owner(s) are  
credited and that the original publication in  
this journal is cited, in accordance with  
accepted academic practice. No use,  
distribution or reproduction is permitted  
which does not comply with these terms.

# Human IL-320A94V mutant attenuates monocyte-endothelial adhesion by suppressing the expression of ICAM-1 and VCAM-1 via binding to cell surface receptor integrin $\alpha V\beta 3$ and $\alpha V\beta 6$ in TNF- $\alpha$ -stimulated HUVECs

Jae-Young Park<sup>1†</sup>, Hyo-Min Park<sup>1†</sup>, Seonhwa Kim<sup>1</sup>,  
Kyeong-Bae Jeon<sup>1</sup>, Chae-Min Lim<sup>1</sup>, Jin Tae Hong<sup>2</sup>  
and Do-Young Yoon<sup>1\*</sup>

<sup>1</sup>Department of Bioscience and Biotechnology, Konkuk University, Seoul, Republic of Korea, <sup>2</sup>College of Pharmacy & Medical Research Center, Chungbuk National University, Cheongju, Republic of Korea

Interleukin-32 (IL-32), first reported in 2005, and its isoforms have been the subject of numerous studies investigating their functions in virus infection, cancer, and inflammation. IL-320, one of the IL-32 isoforms, has been shown to modulate cancer development and inflammatory responses. A recent study identified an IL-320 mutant with a cytosine to thymine replacement at position 281 in breast cancer tissues. It means that alanine was also replaced to valine at position 94 in amino acid sequence (A94V). In this study, we investigated the cell surface receptors of IL-320A94V and evaluated their effect on human umbilical vein endothelial cells (HUVECs). Recombinant human IL-320A94V was expressed, isolated, and purified using Ni-NTA and IL-32 mAb (KU32-52)-coupled agarose columns. We observed that IL-320A94V could bind to the integrins  $\alpha V\beta 3$  and  $\alpha V\beta 6$ , suggesting that integrins act as cell surface receptors for IL-320A94V. IL-320A94V significantly attenuated monocyte-endothelial adhesion by inhibiting the expression of Intercellular adhesion molecule-1 (ICAM-1) and vascular cell adhesion molecule-1 (VCAM-1) in tumor necrosis factor (TNF)- $\alpha$ -stimulated HUVECs. IL-320A94V also reduced the TNF- $\alpha$ -induced phosphorylation of protein kinase B (AKT) and c-jun N-terminal kinases (JNK) by inhibiting phosphorylation of focal adhesion kinase (FAK). Additionally, IL-320A94V regulated the nuclear translocation of nuclear factor kappa B (NF- $\kappa$ B) and activator protein 1 (AP-1), which are involved in ICAM-1 and VCAM-1 expression. Monocyte-endothelial adhesion mediated by ICAM-1 and VCAM-1 is an important early step in atherosclerosis, which is a major cause of cardiovascular disease. Our findings suggest that IL-320A94V binds to the cell surface receptors, integrins

$\alpha V\beta 3$  and  $\alpha V\beta 6$ , and attenuates monocyte-endothelial adhesion by suppressing the expression of ICAM-1 and VCAM-1 in TNF- $\alpha$ -stimulated HUVECs. These results demonstrate that IL-32 $\theta$ A94V can act as an anti-inflammatory cytokine in a chronic inflammatory disease such as atherosclerosis.

#### KEYWORDS

IL-32 $\theta$ , integrins, Intercellular adhesion molecule-1, vascular cell adhesion molecule-1, human umbilical vein endothelial cells, monocyte-endothelial adhesion

## 1 Introduction

IL-32, previously known as NK4, is expressed in activated human T cells and NK cells after stimulation by mitogen or IL-2. Previous studies showed that NK4 induced pro-inflammatory cytokines such as IL-8, TNF- $\alpha$ , and MIP-2 in several immune cells through the classical cytokine signaling pathway, but lacked sequence homology with other cytokines. Hence, it was renamed IL-32, a part of one of the interleukin families (1). Numerous studies have reported that IL-32 is associated with cancer growth and development, viral infections, as well as chronic inflammatory diseases such as Crohn's disease, inflammatory bowel disease, and rheumatoid arthritis, which demonstrated the ability of IL-32 to function as a cytokine (2–12). The IL-32 gene contains eight exons, with several splice variants differing in structure. IL-32 $\alpha$ , IL-32 $\beta$ , IL-32 $\gamma$ , and IL-32 $\delta$  were first discovered in NK cells, with IL-32 $\gamma$  having the longest sequence among the IL-32 isoforms (1). IL-32 $\epsilon$ , IL-32 $\zeta$ , IL-32 $\eta$ , IL-32 $\theta$ , and IL-32sm were additionally identified, and a total of nine isoforms have been reported (13, 14). Early studies on IL-32 suggest that it is a pro-inflammatory cytokine. However, further studies on the individual isoforms show that they play different roles (15).

IL-32 $\theta$ , one of the IL-32 isoforms, is the only isoform with an exon 6 deletion, except for IL-32sm. Recent studies have shown that IL-32 $\theta$  has tumor suppression and anti-inflammatory effects (16, 17). We recently identified mutations in IL-32 $\theta$  in tissues from patients with breast cancer. Sequence analyses revealed a cytosine to thymine replacement at position 281 in the mutant isoform, leading to a change in the amino acid sequence from alanine to valine at position 94 in the protein sequence. The mutant showed anti-inflammatory function inhibiting pro-inflammatory cytokines such as IL-1 $\beta$ , IL-6, IL-8, and COX2 in breast cancer cells (18). Previous studies on IL-32 $\theta$ A94V were limited to overexpression, and its specific receptor was not clearly identified. IL-32 $\alpha$  and IL-32 $\beta$  have been reported to bind to integrin  $\alpha V\beta 3$  and integrin  $\alpha V\beta 6$  (19). In this study, we investigated whether these integrins could also act as receptors for IL-32 $\theta$ A94V.

Intercellular adhesion molecule-1 (ICAM-1) and vascular cell adhesion molecule-1 (VCAM-1) are markers of inflammatory responses involved in various diseases, including asthma and rheumatoid arthritis (20–25). Pro-inflammatory cytokines such as IL-1 $\beta$  and TNF- $\alpha$  (26, 27) induce the expression of ICAM-1 and VCAM-1 in vascular endothelial cells (26, 27). One of their functions is to initiate trans-endothelial migration (TEM) by

arresting monocytes and leukocytes. TEM refers to the process that immune cells adhere to vascular endothelial cells and pass between them to migrate to the inflammation region. This process contribute to enhancement of the inflammatory response (28). ICAM-1 and VCAM-1 bind to lymphocyte function-associated antigen 1 (LFA-1) and very late antigen-4 (VLA-4) expressed in monocytes, triggering TEM by arresting the immune cells on the vascular endothelial cells (29). TEM is also important early stage of atherosclerosis. Atherosclerosis is characterized by inflammation, injured endothelial cells, and the formation of plaques due to the accumulation of oxidized low-density lipoproteins (ox-LDL) (30). Plaques contain vascular endothelial cells, smooth muscle cells, and lipid-containing macrophages known as foam cells. ICAM-1 and VCAM-1 induce TEM of monocytes, and the migrated monocytes develop plaques through uptake of ox-LDL (31, 32). Plaque development obstructs blood flow in vessels in various parts of the body, resulting in fatal disease such as cardiovascular disease (CVD) (33, 34). Therefore, regulation of ICAM-1 and VCAM-1 could be an important target for the treatment of various diseases as well as vascular inflammation (35).

Previous studies have suggested that IL-32 $\beta$  and IL-32 $\gamma$  act as pro-inflammatory cytokines involved in the upregulation of ICAM-1 and VCAM-1 (36, 37). In this study, we identified the cell surface receptors for IL-32 $\theta$ A94V and showed that IL-32 $\theta$ A94V was involved in the expression of ICAM-1 and VCAM-1, similar to other isoforms. Interestingly, IL-32 $\theta$ A94V downregulated the expression of ICAM-1 and VCAM-1 in contrast to other isoforms such as IL-32 $\beta$  and IL-32 $\gamma$  (36, 37). These findings support the differential roles of IL-32 isoforms and demonstrate the therapeutic potential of IL-32 $\theta$ A94V in inflammatory diseases such as atherosclerosis.

## 2 Materials and methods

### 2.1 Expression of human IL-32 $\theta$ A94V

IL-32 $\theta$ A94V coding sequence was synthesized by Bioneer (Daejeon, Korea) using HT-oligo<sup>TM</sup> synthesis. The synthesized DNA sequence was cloned into a pTH24 based TEVSH vector (Addgene, Watertown, MA, USA) using NdeI and AgeI restriction sites and rapid DNA ligation kit (Thermo Fisher Scientific, Waltham, MA, USA). TEVSH was a gift from Helena Berglund (Addgene

plasmid # 125194; <http://n2t.net/addgene:125194>; RRID : Addgene 125194) and confirmed by DNA sequencing (Bionics, Seoul, Korea). The recombinant TEVSH vectors were transformed into DH5 $\alpha$  by heat shock and purified using a mini prep kit (Intron Biotechnology, Sungnam, Korea). The IL-32 $\theta$ A94V expression vectors were transformed into Rosetta strain of *Escherichia coli* by heat shock transformation. Successfully transformed single colony was picked up and cultured at 37°C for 4 h in a 200-rpm incubator in Luria–Bertani (LB) media with ampicillin (100  $\mu$ g/mL). The cultured mixture was transferred to 2.4 L of fresh LB media with ampicillin (100  $\mu$ g/mL) and grown in a 200-rpm incubator at 37°C until it reached an OD<sub>600</sub> of 0.6. IL-32 $\theta$ A94V was induced by adding 0.5 mM IPTG. Cells were grown in a 200-rpm incubator at 16°C for 16 h.

## 2.2 Purification of IL-32 $\theta$ A94V using Ni-NTA and CNBr-activated sepharose 4B columns

After 16 h, the cells were harvested by centrifugation at 8,000 rpm for 10 min at 4°C. The supernatant was discarded, and the pellet was lysed using lysis buffer (50 mM Tris-HCl pH 8.0, 10% glycerol, 0.1% Triton X-100, 1X protease inhibitor cocktail, 2 mM MgCl<sub>2</sub>, 0.1 mg lysozyme) and incubated on ice for 30 min. The lysed cells were sonicated (amplitude 35%, turn on 10 s, turn off 10 s) for 1 min using a sonicator (Sonics & Materials, Inc., Newtown, CT, USA). The lysed cells were centrifuged at 13,000 rpm for 30 min at 4°C, and the supernatant was collected. Ni-NTA resin (Thermo Fisher Scientific) was loaded into a PD-10 column and balanced with equilibration buffer (20 mM Tris-HCl pH 8.0, 200 mM NaCl). The lysate was mixed with 10 mL of equilibration buffer and loaded into the column and washed by washing buffer (20 mM Tris-HCl pH 8.0, 200 mM NaCl, 25 mM imidazole). After washing, elution buffer (20 mM Tris-HCl pH 8.0, 500 mM NaCl, 500 mM imidazole) was loaded into the column and the flow-through buffer containing IL-32 $\theta$ A94V was reloaded into IL-32mAb (KU32-52)-coupled CNBr-activated Sepharose 4B column that was prepared using CNBr-activated Sepharose 4B (Sigma-Aldrich, St. Louis, MO, United States) and monoclonal antibody IL-32 mAb KU32-52 (38). After several washing steps with Tris (pH 8.0), IL-32 $\theta$ A94V was eluted with 100 mM glycine (pH 3.0). The tube receiving the eluted solution contained 1 M of Tris (pH 8.0) with one-tenth of the total volume. The purified IL-32 $\theta$ A94V was dialyzed three times with phosphate-buffered saline (PBS) using spectra/Por membrane (Spectrum Laboratories, Piscataway, NJ, USA) for 2 h each. Absence of endotoxin was evaluated by using polymyxin B (Sigma-Aldrich).

## 2.3 3D structure modeling of IL-32 $\theta$ A94V and IL-32 $\theta$ A94V-integrin binding prediction

The tertiary structure of IL-32 $\theta$ A94V was analyzed by I-TASSER (Iterative Threading ASSEmbly Refinement), which is a hierarchical approach to protein structure prediction and structure-based function annotation. I-TASSER identifies structural templates with

full-length models constructed by template-based fragment assembly simulations. Function insights of the target are then derived by re-threading the 3D models through protein function database. Protein-protein docking prediction was performed using the model with the highest confidence score among the models derived from I-TASSER (39–41). Integrin-IL-32 $\theta$ A94V binding was analyzed using HDock server (<http://hdock.phys.hust.edu.cn>), a protein-protein binding prediction tool. HDock predicts the binding complexes between two proteins using a hybrid docking strategy. Structures of extracellular segments of integrin  $\alpha$ V $\beta$ 3 (PDB ID: 1JV2) and  $\alpha$ V $\beta$ 6 (PDB ID: 5FFG) were provided by protein data bank (PDB). The docking scores are calculated by knowledge-based iterative scoring function ITScorePP or ITScorePR (42–46).

## 2.4 IL-32 $\theta$ A94V-integrin binding assay

MaxiSorp flat-bottomed 96-well plates (Nunc, Roskilde, Denmark) were coated with 1  $\mu$ g/mL of recombinant  $\alpha$ V $\beta$ 3 and  $\alpha$ V $\beta$ 6 integrins (R&D Systems, Minneapolis, MN, USA) diluted in PBS and incubated overnight at 4°C. Next, the wells were blocked with 1% BSA (Invitrogen, Waltham, MA, USA) in PBS at 37°C for 1 h followed by three washing steps with PBS containing 0.05% Tween 20. Subsequently, some wells were preincubated with 10  $\mu$ M cyclo-RGDfV peptide (Peptide Institute Inc, Osaka, Japan) or 10% fetal bovine serum (FBS), whereas others were incubated with PBS at 37°C for 1 h. Next, the wells were incubated with various concentrations of mutant IL-32 $\theta$ A94V diluted in PBS, with or without 10  $\mu$ M cyclo-(RGDfV) or 10% FBS at 37°C for 1 h. The wells were washed three times with wash buffer and incubated with IL-32 mAb KU32-52 diluted in PBS at a concentration of 0.2  $\mu$ g/mL at 25°C for 1 h. After the incubation, the wells were washed three times with wash buffer and incubated with mouse-IgGk light chain binding protein conjugated to HRP (m-IgGk BP-HRP) (BETHYL, Waltham, MA USA) at 25°C for 1 h. Next, the wells were washed three times with wash buffer and incubated with TMB substrate at 25°C for 20 min, and the color reaction was stopped with 2.5 N H<sub>2</sub>SO<sub>4</sub>. The absorbance/optical density was measured at 450 nm using a microplate reader (Apollo LB 9110, Berthold Technologies GmbH, Bad Wildbad, Germany).

## 2.5 Cell culture

HUVEC cells were cultured in Dulbecco modified Eagle medium (Welgene Incorporation, Daegu, Korea) supplemented with 10% (v/v) heat-inactivated fetal bovine serum (Hyclone Laboratories, Logan, UT, USA), penicillin (100 U/mL), and streptomycin (100  $\mu$ g/mL). The cells were incubated in a 5% CO<sub>2</sub>-containing chamber at 37°C.

## 2.6 RNA extraction and reverse-transcription polymerase chain reaction (RT-PCR)

HUVEC cells ( $3 \times 10^5$  cells/well) were incubated in 6-well plates for 24 h and starved for 4 h with serum-free media. Subsequently, the cells

were pre-treated with IL-320A94V (10 ng/mL) for 1 h and treated with TNF- $\alpha$  (10 ng/mL) for another 4 h. The treated cells were collected and lysed using the easy-BLUE<sup>TM</sup> Total RNA extraction kit (iNtRon Biotechnology, Seoul, South Korea) according to the manufacturer's instructions. For reverse-transcription (RT) polymerase chain reaction (PCR), RNA (1  $\mu$ g) was reverse-transcribed to cDNA using oligo (dT) primers and M-MuLV reverse transcriptase (New England Biolabs, Ipswich, MA, USA). The synthesized cDNA was amplified using a PCR Thermal Cycler Dice instrument (Takara, Otsu, Shiga, Japan). The following sets of primers were used: integrin  $\alpha$ V, 5'-AGGAGAA GGTGCCTACGAAGCT-3' (forward) and 5'-GCA CAGGAAA GTCTTGCTAAGGC-3' (reverse); integrin  $\beta$ 3, 5'-CATGGATTC CAGCAATGTCCTC C-3' (forward) and 5'-TTGAGGCAGGTG GCATTGAAGG-3' (reverse); integrin  $\beta$ 6, 5'- TCTCCTGCGTGA GACACAAAGG-3' (forward), and 5'-GAGCACTCCATCTT CAGAGACG-3' (reverse); ICAM-1, 5'-AGCGGCTGACG TGTGCAGTAAT-3' (forward), 5'- TCTGAGACCTCTGGC TTCGTCA-3' (reverse); VCAM-1, 5'-GATTCTGTGCC CACAGTAAGG C-3' (forward) and 5'-TGGTCACAGAGC CACCTTCTTG-3' (reverse); glyceraldehyde 3-phosphate dehydrogenase (GAPDH), 5'-AGAACATCATCCCTGCCTCT-3' (forward), 5'-CTGCTT CACCACCTTCTTGA-3' (reverse). GAPDH was used as an internal control. The PCR products were separated on a 2% agarose gel.

## 2.7 Reverse transcription-quantitative polymerase chain reaction (RT-qPCR)

HUVECs were harvested after treatment with or without IL-320A94V and TNF- $\alpha$ . mRNA extraction and cDNA synthesis were performed as described above. RT-PCR was performed with a relative quantification protocol using Rotor-Gene 6000 series software 1.7 (Qiagen, Hilden, Germany) and the Sensi FAST<sup>TM</sup> SYBR NO-ROX Kit (BIOLINE, London, UK). The expression of all target genes was normalized to that of the housekeeping gene, GAPDH. Each sample was run with the following primer sets: ICAM-1, 5'-AGCGGCTGACGTGTGCAGTAAT-3' (forward), 5'-TCTGAGACCTCT GGCTTCGTCA-3' (reverse); VCAM-1, 5'-GATTCTGTGCCCCACAGTAAGG C-3' (forward), 5'-TGG TCACAGAGCCACCTTCTTG-3' (reverse); GAPDH, 5'-AGAAC ATCATCCCTGCCTCT-3' (forward), 5'-CTGCTTACCACCT TCTTGA-3' (reverse). GAPDH was used as an internal control. The mRNA levels of each gene were calculated relative to that of the internal reference, GAPDH using the comparative Ct method (47).

## 2.8 Immunoblotting

HUVEC cells ( $3 \times 10^5$  cells/well) were seeded in 6-well plates for 24 h and pre-treated for 1 h with IL-320A94V (100 ng/mL), followed by treatment with TNF- $\alpha$  (10 ng/mL). The cells were lysed in a buffer containing 50 mM Tris (pH 7.4), 150 mM NaCl, 1% NP-40, 0.1% sodium dodecyl sulfate (SDS), 0.25% sodium deoxycholate, 1 mM ethylene diamine tetraacetic acid (EDTA), 1 mM ethylene glycol tetraacetic acid, 1 mM orthovanadate, aprotinin (10  $\mu$ g/mL), and 0.4

mM phenyl methylsulfonyl fluoride (PMSF) at 4°C for 2 h. The cells were lysed, and the protein content was estimated using a Bradford assay reagent (Bio-Rad Laboratories, Hercules, CA, USA) and UV spectrophotometer (48). The proteins (30  $\mu$ g) were separated on 10% SDS-polyacrylamide gels and transferred to PVDF membranes. The membranes were blocked with 5% skim milk for 1 h at 25°C and incubated with primary antibodies against IL-32, His-tag (Sigma-Aldrich), FAK (Thermo Fisher Scientific), AKT (Cell Signaling, Danvers, MA, USA), JNK (Cell Signaling), I $\kappa$ B (Cell Signaling), p65 (Cell Signaling), p50 (Cell Signaling), PARP (Cell Signaling), c-Jun (Santa Cruz Biotechnology, Dallas, TX, USA), and c-Fos (Santa Cruz Biotechnology), for 1 h at 25°C. After incubation, the membranes were incubated with secondary antibodies (anti-rabbit or anti-mouse IgG antibodies) (BETHYL) for 1 h at 25°C. Finally, the protein bands were visualized using an enhanced chemiluminescence Western blotting detection kit (Advanta, San Jose, CA USA).

## 2.9 Immunofluorescence

HUVEC cells ( $1.0 \times 10^5$  cells/well) were seeded in an 8-well slide chamber for 24 h and starved overnight, followed by pre-treatment for 1 h with IL-320A94V (100 ng/mL) and a 6 h treatment with TNF- $\alpha$  (10 ng/mL). After the treatment, cells were fixed using 4% paraformaldehyde for 10 min followed by incubation with ice-cold methanol and blocking using 1% BSA in PBS for 1 h at 25°C. The cells were then incubated with primary antibodies against ICAM-1 and VCAM-1 (Beijing Solarbio Science & Technology Co., Beijing, China) overnight at 4°C, and with secondary antibodies conjugated to Cy3 (Merck Millipore, Darmstadt, Germany) for 1 h at 25°C, followed by DAPI staining. Two washing steps with PBS were performed between each step. Thereafter, cells were mounted in mounting buffer (Sigma-Aldrich) and examined under a fluorescence microscope.

## 2.10 siRNA transfection

HUVEC cells ( $3 \times 10^5$  cells/well) were seeded in 6-well plates for 24 h and changed to fresh media. For silencing ICAM-1 and VCAM-1 expression, cells were transfected with the following siRNA sets (Bionics, Seoul, Korea): NC, 5'-UUCUCCGAACGUGUCACGUTT-3'; ICAM-1, 5'-UUCUUGUGUAUAAGCUGGCCGTT-3'; VCAM-1, 5'-CCAUUGUUCUCAUGGAGAATT-3'; (49, 50). INTERFERin reagent (Polyplus, Illkirch, France) was used for transfection, according to the manufacturer's instruction. The final siRNA concentrations were 1 nM (VCAM-1) and 5 nM (ICAM-1), respectively. After 24 h of transfection, the cells were starved for 4 h followed by treatment with TNF- $\alpha$  (10 ng/mL) for another 4 h. The silencing efficiency was measured by RT-PCR analysis.

## 2.11 Monocyte-endothelial cell adhesion assay

HUVEC cells ( $1.5 \times 10^5$  cells/well) were seeded in a 4-well slide chamber for 24 h and starved overnight, pre-treated with IL-320A94V

(100 ng/mL) for 1 h, followed by 6 h treatment with TNF- $\alpha$  (10 ng/mL). The THP-1 cells were labeled with 5  $\mu$ M calcein-AM (Molecular Probes, Eugene, OR, USA) for 30 min in RPMI-1640 without FBS. The THP-1 cells labeled with calcein-AM were added to the 4-well slide chamber containing the HUVECs and incubated for 30 min in RPMI-1640 containing 10% FBS. Subsequently, unbound monocytes were removed by three washes with PBS. Remaining monocytes were determined using a fluorescence microscope. The intensity of fluorescence was measured using ImageJ software version 1.5 (51).

## 2.12 Preparation of cytosol and nuclear extracts

HUVEC cells ( $2.5 \times 10^5$  cells/dish) were seeded in a cell culture dish for 24 h, pre-treated with IL-320A94V (100 ng/mL) for 1 h, and treated with TNF- $\alpha$  (10 ng/mL) for 30 min before harvesting and fractionating using NE-PER nuclear and cytoplasmic extraction reagents (Thermo Fisher Scientific) according to the manufacturer's instructions. Equal quantities of protein from these extracts (50  $\mu$ g) were separated by SDS-polyacrylamide gel electrophoresis and transferred to PVDF membranes. The subsequent steps for the procedure were followed as described for Western blotting above. PARP was used as a nuclear protein marker.

## 3 Results

### 3.1 Expression and purification of recombinant human IL-320A94V

TEVSH vector was used for expression of IL-320A94V, and recombinant IL-320A94V DNA was inserted into the vector by NdeI and AgeI restriction enzymes. The TEVSH vector contained a His tag for protein purification. A schematic diagram of the recombinant vector is shown in Figure 1A. We performed consecutive purifications to improve the purity of IL-320A94V. First, IL-320A94V was separated by binding on a Ni-NTA column and His tag, and the separated IL-320A94V was purified once more by a CNBr-activated Sepharose 4B column coupled with IL-32mAb KU32. Purified IL-320A94V was analyzed using SDS-PAGE (Figure 1B) and Western blots (Figures 1C, D). In SDS-PAGE analysis, no other notable protein bands were detected except for IL-320A94V in the eluate of the Ni-NTA column, but several other proteins were observed using Western blotting. These non-target proteins were removed by further purification using CNBr-activated Sepharose 4B column coupled to KU32-52. In the end, highly pure IL-320A94V protein was obtained with few other proteins.

### 3.2 Binding of IL-320A94V to integrin $\alpha$ V $\beta$ 3 and $\alpha$ V $\beta$ 6

We predicted the binding of IL-320A94V to integrins using the HDOCK server. IL-320A94V was indicated as a yellow molecule containing a helix structure, and the extracellular domain of integrin  $\alpha$ V $\beta$ 3 and  $\alpha$ V $\beta$ 6 provided from PDB were indicated as

orange molecules. The binding score of IL-320A94V-integrin  $\alpha$ V $\beta$ 3 was -304.56, and the confidence score was 0.9565. The binding score of IL-320A94V-integrin  $\alpha$ V $\beta$ 6 was -358.20, and the confidence score was 0.9847, which was higher than that of IL-320A94V-integrin  $\alpha$ V $\beta$ 3 (Figure 2).

In addition to structure-based binding prediction (Figure 2), we also performed an IL-320A94V-integrin binding assay (Figure 3). After coating 96-well plates with integrin  $\alpha$ V $\beta$ 3 and  $\alpha$ V $\beta$ 6, IL-320A94V was added at the concentration shown in Figure 3A. In the presence of the integrins, the absorbance increased in a concentration-dependent manner of IL-320A94V but not in BSA (Figure 3A), indicating that IL-320A94V also binds to the integrins  $\alpha$ V $\beta$ 3 and  $\alpha$ V $\beta$ 6 similar to other isoforms. Cyclo-RGDfV, which is known to bind to the RGD-binding site of integrins, was pretreated in 96-well plates, and PBS was used as a control. Further, wells were coated with integrins  $\alpha$ V $\beta$ 3 and  $\alpha$ V $\beta$ 6. IL-320A94V was treated at the concentrations shown in Figure 3B. In both integrins  $\alpha$ V $\beta$ 3 and  $\alpha$ V $\beta$ 6, integrin-IL-320A94V binding was not significantly reduced by cyclo-(RGDfV) (Figure 3B), suggesting that IL-320A94V binds to the non-RGD binding sites. In the other group, media containing 10% FBS were pretreated in 96-well plates. Integrins  $\alpha$ V $\beta$ 3 and  $\alpha$ V $\beta$ 6 were then added, and the control group was pretreated with serum-free media. IL-320A94V was treated at the concentrations shown in Figure 3C. In contrast to cyclo-(RGDfV), integrin-IL-320A94V binding was significantly inhibited by FBS (Figure 3C). These results demonstrated that IL-320A94V binds to the non-RGD binding site of integrin  $\alpha$ V $\beta$ 3 and  $\alpha$ V $\beta$ 6, similar to other isoforms such as IL-32 $\beta$ , and suggest that these integrins can act as cell surface receptors for IL-320A94V.

### 3.3 Effects of IL-320A94V on expression of ICAM-1 and VCAM-1 in TNF- $\alpha$ -stimulated HUVEC cells

We confirmed the expression of integrins in HUVECs to evaluate the effects of IL-320A94V on cells. THP-1 monocytes were used as a negative control, which did not express integrin  $\alpha$ V $\beta$ 3 and  $\alpha$ V $\beta$ 6 on their surfaces (Figure 4A). And, we investigated the effect of IL-320A94V on the expression of ICAM-1 and VCAM-1 in TNF- $\alpha$ -stimulated HUVEC cells. HUVECs were starved for 4 h to minimize the interference by FBS, and IL-320A94V was pretreated for 1 h and stimulated with TNF- $\alpha$  for 4 h or 6 h. The mRNA levels of ICAM-1 and VCAM-1 were measured using RT-PCR (Figure 4B) and RT-qPCR (Figure 4C). mRNA expression levels of ICAM-1 and VCAM-1 were increased by TNF- $\alpha$  and significantly decreased by IL-320A94V. The protein expressions were also analyzed using immunofluorescence. The fluorescence intensities of ICAM-1 and VCAM-1 were increased upon TNF- $\alpha$  stimulation and suppressed by IL-320A94V as expected (Figure 5).

### 3.4 Effects of IL-320A94V on monocyte-endothelial cell adhesion

As LFA-1 and VLA-4 are known to bind ICAM-1 and VCAM-1, respectively, we confirmed the expression of LFA-1

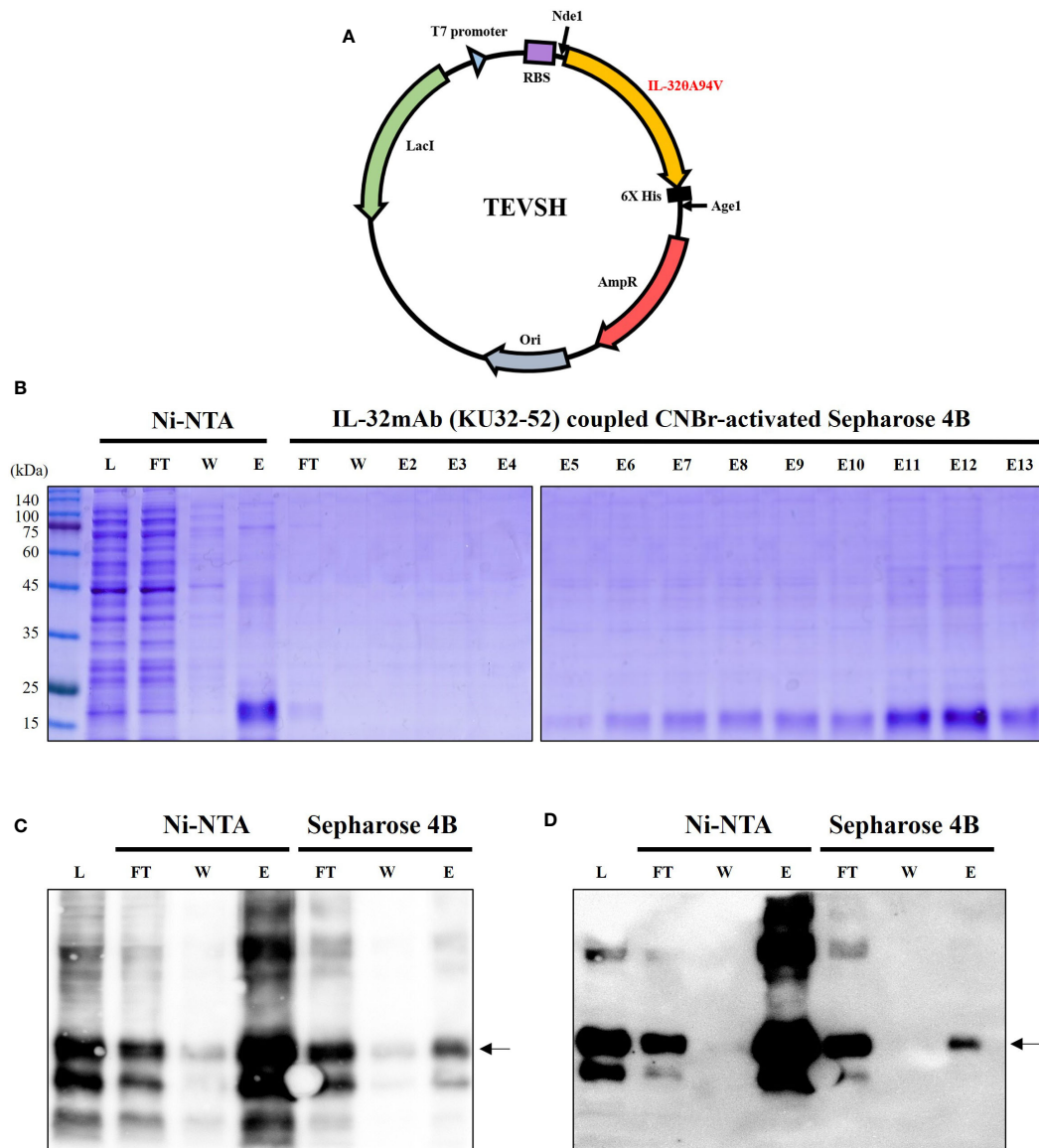
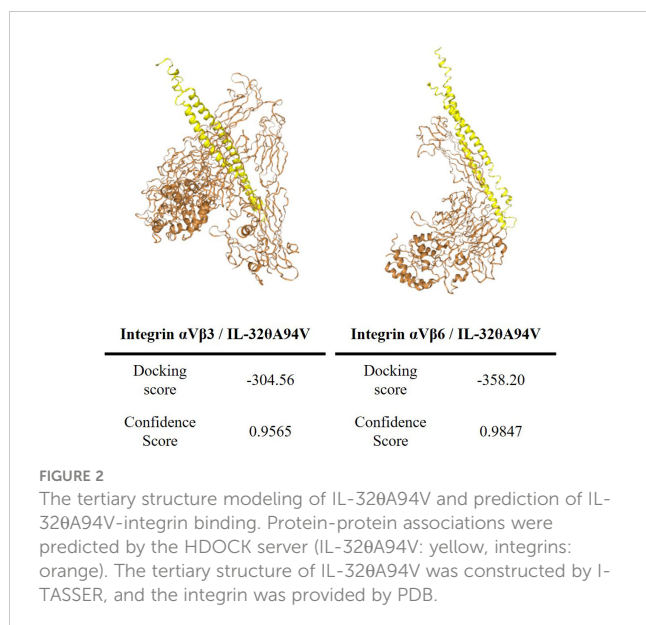


FIGURE 1

Expression and purification of IL-320A94V. (A) Schematic diagram of mutant IL-320A94V expression vector. As a protein expression vector, TEVSH with pTH24 as a backbone was used. His tag was included for purification. NdeI, AgeI restriction enzymes were used to construct recombinant DNA. SDS-PAGE (B) and Western blot using KU32-52 mAb (C) or anti-His tag mAb (D) were performed to confirm the isolated protein. IL-320A94V was purified twice by Ni-NTA column followed by IL-32mAb (KU32-52) coupled CNBr-activated Sepharose 4B. IL-320A94V bound to Ni-NTA column was eluted with 500 mM imidazole, and further purification was performed by IL-32 mAb (KU32-52)-coupled CNBr-activated Sepharose 4B using low pH Tris-glycine buffer (pH 3.0). L, lysate of *Escherichia coli* harboring IL-320A94V expression vector; FT, flow through; W, washing flow; E, elution; E2-E13, eluted using low pH Tris-glycine buffer (pH 3.0).

and VLA-4 in THP-1 cells. Expression of these molecules implies that THP-1 can attach to HUVECs through the interaction of ICAM-1 and VCAM-1. Additionally, the expression of LFA-1 and VLA-4 was not reduced by treatment of IL-320A94V (Figure 6A). We used siRNA transfection to verify whether downregulation of ICAM-1 and VCAM-1 leads to suppression of monocyte-endothelial adhesion. The mRNA levels of TNF- $\alpha$ -induced ICAM-1 and VCAM-1 were reduced by siRNA transfection (Figure 6B). In co-cultures of THP-1 cells and HUVECs, residual calcein-AM-labeled THP-1 (green) was increased by TNF- $\alpha$  and attenuated by siRNA transfection

(Figure 6C). These results suggest that the monocyte-endothelial adhesion was regulated by the expression levels of ICAM-1 and VCAM-1. Previously, in Figure 4 and 5, we found that IL-320A94V inhibited ICAM-1 and VCAM-1 expression. Thus, we investigated whether IL-320A94V could attenuate monocyte-endothelial adhesion. Adhesion between calcein-AM-labeled THP-1 and HUVECs was increased by TNF- $\alpha$  and significantly suppressed by IL-320A94V (Figure 6D). Taken together, it was suggested that IL-320A94V attenuated monocyte-endothelial adhesion by inhibiting the expression of ICAM-1 and VCAM-1 in TNF- $\alpha$ -stimulated HUVECs.



### 3.5 Effects of IL-320A94V on phosphorylation levels of FAK, AKT, and JNK in TNF- $\alpha$ -stimulated HUVEC cells

We revealed that IL-320A94V inhibited the expression of ICAM-1 and VCAM-1 in TNF- $\alpha$ -stimulated HUVECs. We performed Western blot to identify the intracellular signaling pathway underlying the regulation of ICAM-1 and VCAM-1 expression mediated by IL-320A94V. IL-320A94V significantly reduced the phosphorylation level of TNF- $\alpha$ -induced focal adhesion kinase (FAK), a well-known integrin-mediated signaling molecule, which is an upstream molecule of protein kinase B (AKT) and c-Jun N-terminal kinase (JNK). IL-320A94V also downregulated phosphorylation levels of AKT and JNK by inhibiting FAK, as expected (Figure 7).

### 3.6 Effects of IL-320A94V on nuclear translocation of NF- $\kappa$ B and AP-1 in TNF- $\alpha$ -stimulated HUVEC cells

TNF- $\alpha$  stimulation activates the FAK/AKT signaling pathway, leading to nuclear translocation of NF- $\kappa$ B (p65/p50) via phosphorylation of I $\kappa$ B. In addition, activation of JNK accelerates nuclear translocation of AP-1 (c-fos/c-jun). These transcription factors promote the expression of ICAM-1 and VCAM-1 (52, 53). We confirmed the phosphorylation level of I $\kappa$ B and nuclear translocation of NF- $\kappa$ B (p65/p50) and AP-1 (c-Fos/c-Jun). IL-320A94V marginally attenuated the TNF- $\alpha$ -induced I $\kappa$ B phosphorylation (Figure 8A). Nuclear translocation of AP-1 (c-Fos/c-Jun) and NF- $\kappa$ B (p65/p50) was increased by TNF- $\alpha$  stimulation and was inhibited by IL-320A94V (Figure 8B). These

results show that IL-320A94V regulated the nuclear translocation of AP-1 (c-Fos/c-Jun) and NF- $\kappa$ B (p65/p50) in TNF- $\alpha$ -stimulated HUVECs, which in turn results in the attenuation of ICAM-1 and VCAM-1 expression.

## 4 Discussion

IL-32 is involved in various cell functions such as apoptosis, differentiation, viral infection, and modulation of inflammatory cytokines, indicating that it is a cytokine that plays key roles in several diseases. However, the role of IL-32 isoforms can vary depending on experimental conditions such as cell lines or diseases. Previous studies on IL-32 suggest the necessity to define the various functions of IL-32 isoforms. For example, IL-32 $\alpha$  and IL-32 $\beta$  are cytokines with both pro- and anti-inflammatory properties (54–57). IL-32 $\gamma$  has mainly pro-inflammatory properties by inducing pro-inflammatory cytokines such as IL-6, IL-12, and CCL5 (58, 59). IL-32 $\theta$  is known to have anti-inflammatory and tumor suppression properties (60, 61).

Recently, an IL-320A94V mutant was discovered in the tissues from a patient with breast cancer, and IL-320A94V was found to suppress the expression of pro-inflammatory cytokines in breast cancer cells (18). Wild type IL-32 $\theta$  recombinant protein has been reported to have the most dominant biological activity among the seven IL-32 isoforms. It significantly increased IL-6, IL-8 and TNF- $\alpha$  in various cells (62). However, in this study, we purified a recombinant IL-320A94V protein and investigated whether a IL-32 $\theta$  mutant would possess the anti-inflammatory effects mediated via cell surface receptors as an exogenous modulator.

We designed a recombinant vector using NdeI and AgeI restriction enzymes (Figure 1A). The vector was transformed into *Rosetta*, one of the strains of *E. coli*, by the heat-shock method. The insert DNA contained a His-tag for purification. We obtained pure IL-320A94V using sequential purification of Ni-NTA column and an IL-32 mAb KU32-52 coupled CNBr-activated Sepharose 4B column. Purified proteins were confirmed by SDS-PAGE (Figure 1B) and Western blot (Figures 1C, D).

Most IL-32 isoforms, including IL-320A94V, have an RGD motif, and integrin  $\alpha V\beta 3$  and  $\alpha V\beta 6$  are known to bind to the RGD motif. In addition, it was reported that these integrins bind to IL-32 $\alpha$  and IL-32 $\beta$  (19). Thus, we hypothesized that IL-320A94V would also bind to these integrins, and analyzed using protein-protein binding prediction tool, HDock server. According to the description of the HDock server, protein-protein binding typically has a score of -200 or higher, more negative docking score means a more possible binding model. Also, confidence score of 0.7 or higher means that the two molecules are highly likely to bind at -200 or higher docking score (42–46). Therefore, the result of docking prediction suggests that IL-320A94V has strong binding potential with integrin  $\alpha V\beta 3$  and integrin  $\alpha V\beta 6$ . IL-320A94V showed a higher docking score with integrin  $\alpha V\beta 6$  than integrin  $\alpha V\beta 3$  (Figure 2). However, no significant difference was identified in the IL-320A94V-integrin binding assay. IL-320A94V was found to bind to both integrin  $\alpha V\beta 3$  and  $\alpha V\beta 6$  in a dose dependent manner (Figure 3A), suggesting that these integrins can act as

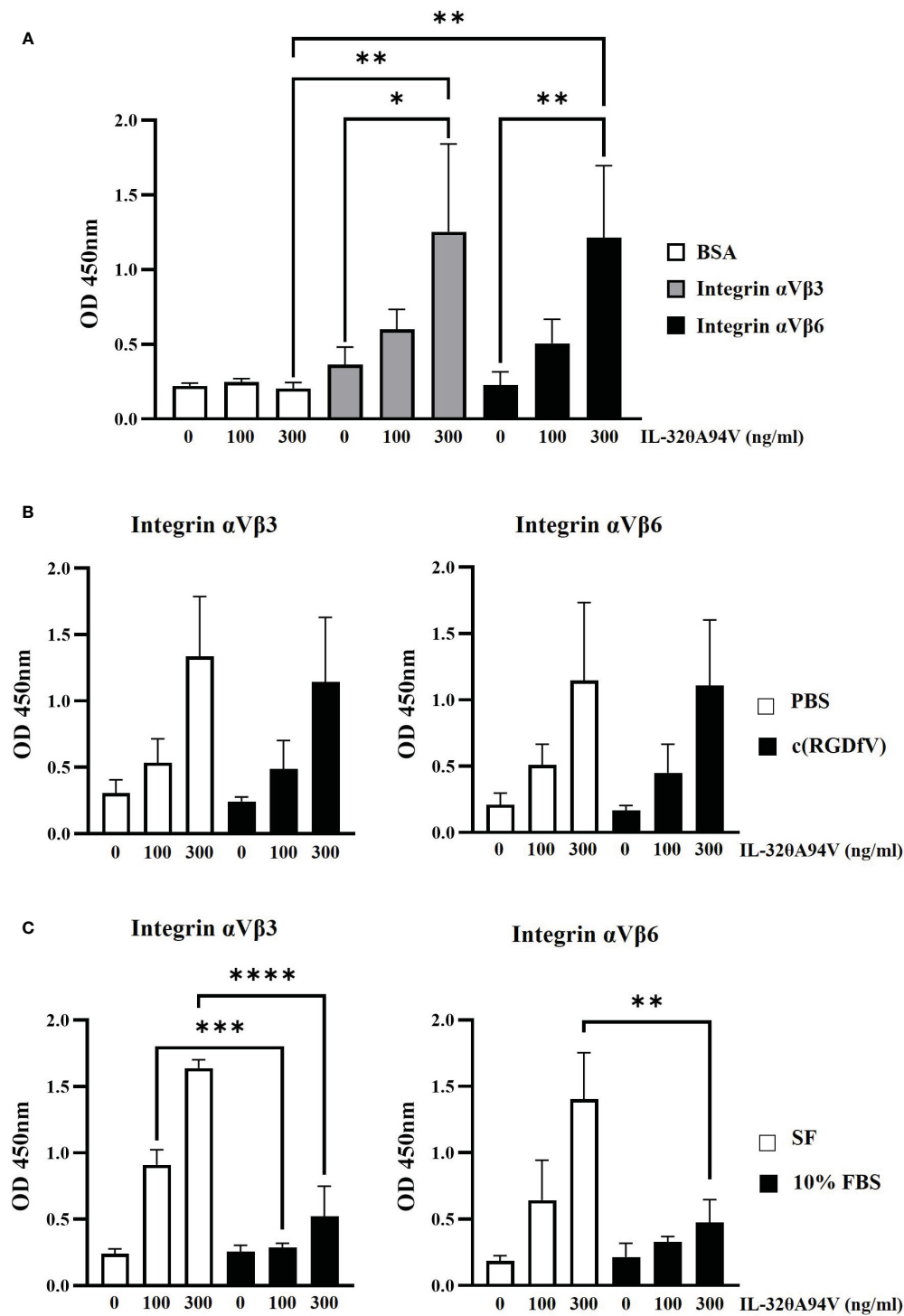
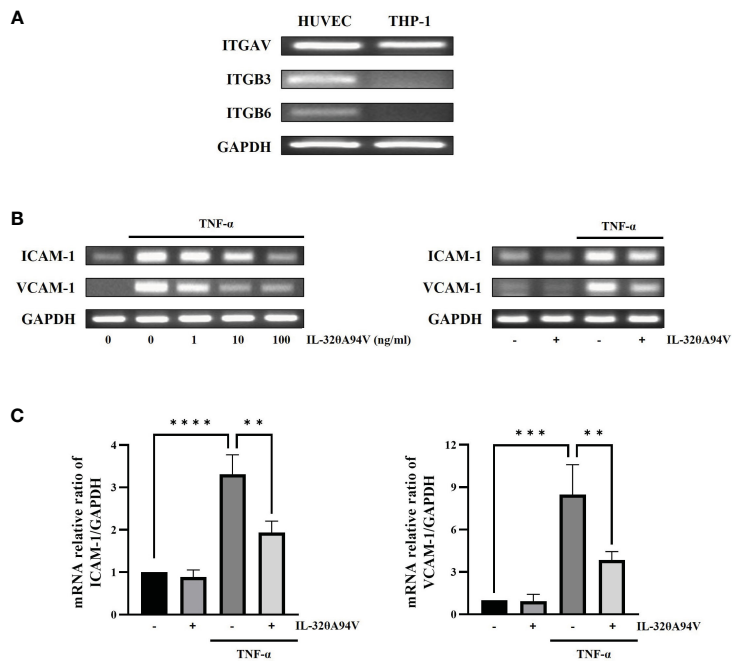


FIGURE 3

IL-320A94V binding to recombinant  $\alpha V\beta 3$  and  $\alpha V\beta 6$  integrins. (A) IL-320A94V binds to the recombinant  $\alpha V\beta 3$  and  $\alpha V\beta 6$  integrins. The effects of cyclo-(RGDFV) (B) and FBS (C) on the bindings between IL-320A94V and recombinant  $\alpha V\beta 3$  or  $\alpha V\beta 6$  integrins were assessed using IL-32 mAb (KU32-52). The results represent the mean  $\pm$  SD of three experiments (\* $p$  < 0.05, \*\* $p$  < 0.01, \*\*\* $p$  < 0.001, \*\*\*\* $p$  < 0.0001 by one-way ANOVA).

receptors for IL-320A94V. However, the interaction was not blocked by cyclo-(RGDFV), including the short RGD peptide, indicating that, contrary to expectations, IL-320A94V-integrin binding is not mediated by the RGD motif (Figure 3B). Extracellular matrix such as fibronectin, vitronectin, and growth

factors included in FBS are known to bind to integrins (63–65). They can block an integrin-IL-320A94V interaction by binding to integrins. We observed that the interaction was reduced in a 10% FBS-containing medium compared to that in the serum free media, as expected (Figure 3C).



**FIGURE 4**  
 The effect of IL-320A94V on mRNA expression of ICAM-1 and VCAM-1 in TNF-α stimulated human umbilical vein endothelial cells (HUVECs). (A) The expression of integrins αV, β3 and β6 subunits were confirmed by RT-PCR in HUVEC cells but not in THP-1 human monocytic cells. HUVECs were pre-treated with IL-320A94V (100 ng/mL) for 1 h and stimulated with TNF-α (10 ng/mL) for 4 h. mRNA expression of adhesion molecules was detected by RT-PCR (B) and RT-qPCR (C) analyses. The results represent the mean ± SD of three experiments (\*\* p < 0.01, \*\*\* p < 0.001, \*\*\*\* p < 0.0001 by one-way ANOVA).

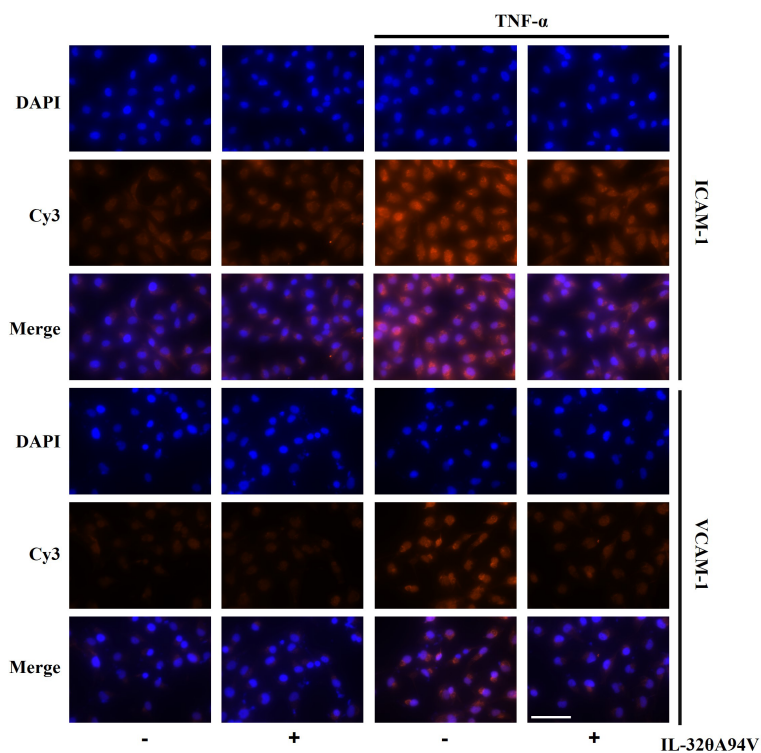


**FIGURE 5**  
 The effect of IL-320A94V on protein expression of ICAM-1 and VCAM-1 in TNF-α stimulated human umbilical vein endothelial cells (HUVECs). HUVECs were pre-treated with IL-320A94V (100 ng/mL) for 1 h and stimulated with TNF-α (10 ng/mL) for 6 h. Protein expression of adhesion molecules was analyzed by immunofluorescence using specific antibodies. Scale bar in each image represents 75 μm.

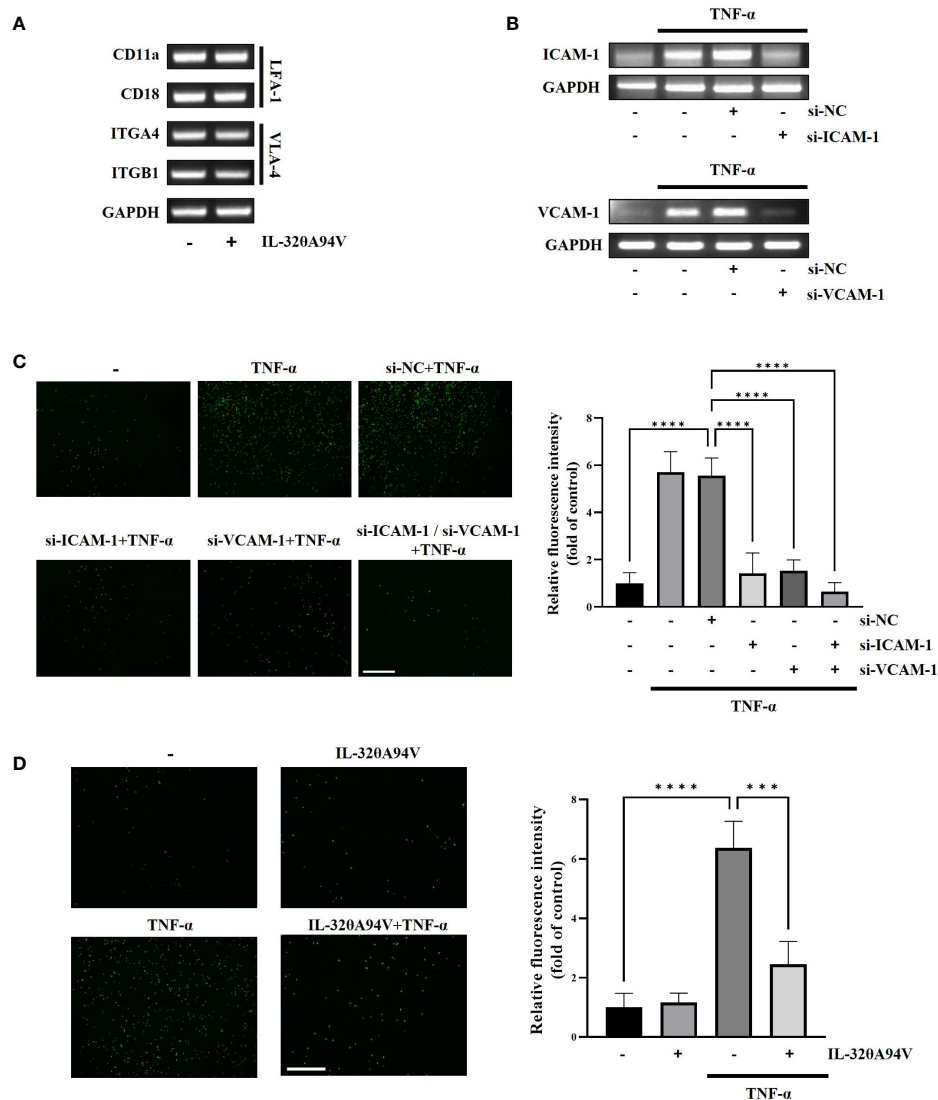


FIGURE 6

IL-320A94V attenuates monocyte adhesion to HUVECs. (A) THP-1 cells were treated with IL-320A94V (100 ng/ml) for 24 h. LFA-1 (CD11a/CD18) and VLA-4 (ITGA4/ITGB1) expression in THP-1 cells was confirmed by RT-PCR analysis. (B) HUVECs were transfected with siRNA for 24 h followed by starved 4 h, then, treated with TNF- $\alpha$  for 4 h. siRNA transfection efficiency was evaluated by RT-PCR analysis. (C, D) Fluorographs of calcein-AM-labeled THP-1 cell attachment to HUVECs. HUVECs were incubated with calcein-AM-labeled THP-1 for 30 min after treatment or transfection as shown in figure. Fluorescence was measured using ImageJ software. Quantified fluorescence intensity was normalized to the control. Scale bar in each image represents 650  $\mu$ m. The results represent the mean  $\pm$  SD of three experiments (\*\* $p$  < 0.001, \*\*\*\*  $p$  < 0.0001 by one-way ANOVA).

RT-PCR analyses confirmed the expression of integrins  $\alpha$ V $\beta$ 3 and  $\alpha$ V $\beta$ 6 in HUVEC cells but not in THP-1 human monocytic cells. We also demonstrated that TNF- $\alpha$ -induced upregulation of ICAM-1 and VCAM-1 expression was significantly decreased in IL-320A94V-pretreated HUVECs (Figures 4, 5). These results show an opposite role of IL-320A94V, compared to IL-32 $\beta$  and IL-32 $\gamma$ , which are known to induce the expression of these cell adhesion molecules (36, 37).

We confirmed that monocyte-endothelial adhesion was mediated by ICAM-1 and VCAM-1 using siRNA transfection (Figures 6B, C). Further, we investigated whether IL-320A94V attenuated monocyte-endothelial adhesion by suppressing expression of these cell adhesion molecules. THP-1 monocytes

were stained with the fluorescent dye calcein-AM and co-cultured with HUVECs. After several washes, the green staining fluorescence intensity of TNF- $\alpha$ -treated THP-1 cells was significantly enhanced, while fluorescence intensity of monocytes was reduced by IL-320A94V (Figure 6D). These results demonstrated that IL-320A94V attenuates monocyte endothelial adhesion by inhibiting the expression of cell adhesion molecules, ICAM-1 and VCAM-1, in TNF- $\alpha$ -stimulated HUVECs.

FAK is a well-known integrin-mediated signaling molecule, which is closely involved in intracellular signals induced by various cytokines and growth factors (66). Phosphorylated FAK induced by these molecules activates the AKT and JNK signaling pathways (67, 68). Activation of AKT induces phosphorylation of

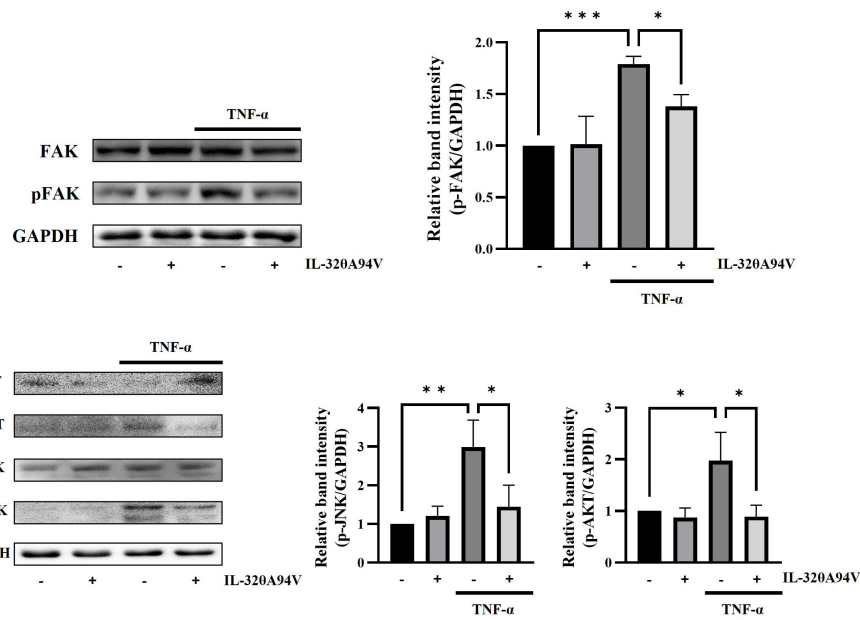


**FIGURE 7** Effect of IL-320A94V on phosphorylation level of FAK, JNK, and AKT in HUVEC cells. HUVECs were pre-treated with IL-320A94V (100 ng/mL) for 1 h followed by stimulation with TNF- $\alpha$  for 10 min (FAK) or 15 min (JNK, AKT). Phosphorylation levels of FAK, AKT, and JNK were confirmed by Western blot, and band intensities were quantified using ImageJ software. The results represent the mean  $\pm$  SD of three experiments (\* $p$  < 0.05, \*\*  $p$  < 0.01, \*\*\*  $p$  < 0.001 by one-way ANOVA).

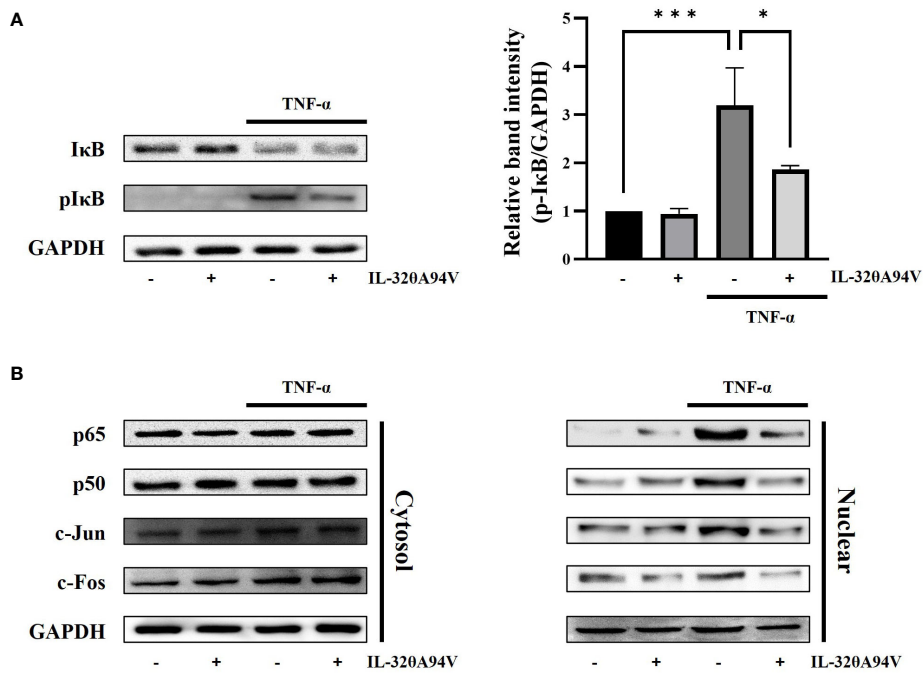


**FIGURE 8** The effect of IL-320A94V on phosphorylation levels of I $\kappa$ B and nuclear translocation of NF- $\kappa$ B (p65/p50), AP-1 (c-Fos/c-Jun) in HUVEC cells. HUVEC cells were incubated with IL-320A94V for 1 h, then stimulated with TNF- $\alpha$  (10 ng/ml) for another 10 min (I $\kappa$ B) or 30 min (transcription factors). Harvested cells were subjected to nuclear fractionation. Phosphorylation and translocation levels were analyzed by Western blot, and band intensities were quantified using ImageJ software. The results represent the mean  $\pm$  SD of three experiments (\* $p$  < 0.05, \*\*\*  $p$  < 0.001 by one-way ANOVA).

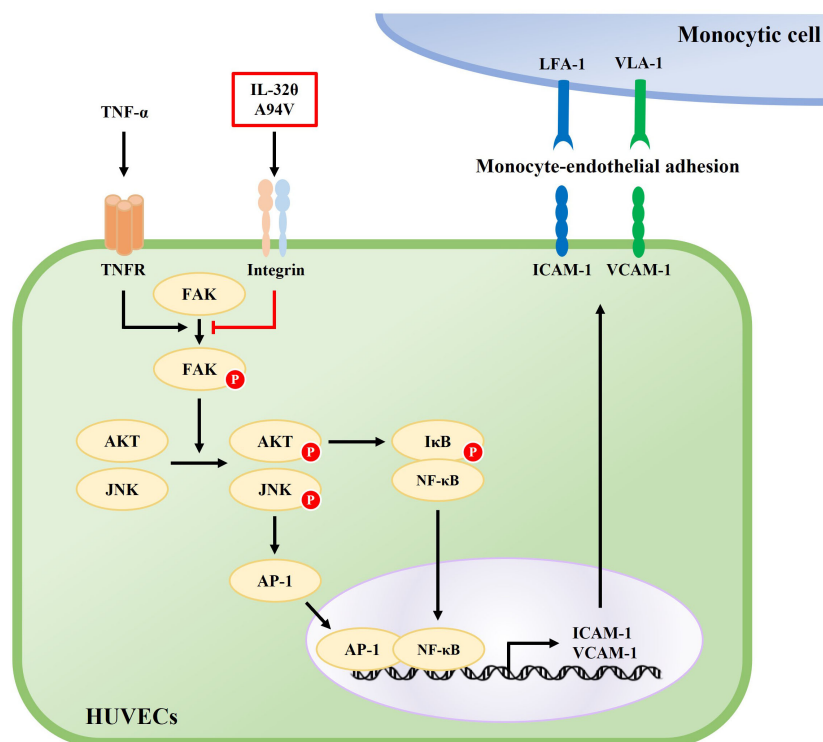


FIGURE 9

Schematic diagram of the effect of IL-32A94V on the TNF- $\alpha$ -induced ICAM-1 and VCAM-1 expression signaling pathway. TNF- $\alpha$ -induced phosphorylation of FAK, AKT, JNK, and nuclear translocation of NF- $\kappa$ B, AP-1 promotes the expression of ICAM-1 and VCAM-1. IL-32A94V inhibits the expression of ICAM-1 and VCAM-1 by inhibiting these intracellular signaling pathways.

I $\kappa$ B, which promotes nuclear translocation of NF- $\kappa$ B. JNK also triggers nuclear translocation of AP-1. The expression of ICAM-1 and VCAM-1 in HUVECs is accelerated by the transcription factors AP-1 and NF- $\kappa$ B (52, 53). IL-32A94V downregulated this signaling pathway by inhibiting TNF- $\alpha$ -induced phosphorylation of FAK, which lies upstream of JNK and AKT, thus attenuating ICAM-1 and VCAM-1 expression (Figures 7, 8).

Increasing evidence suggests that ICAM-1 and VCAM-1 enhance the inflammatory response and are involved in various diseases (69–72). It has been well known that ICAM-1 and VCAM-1 play roles in arresting immune cells and initiating TEM, which plays an essential step in the development of atherosclerosis. Atherosclerosis, a chronic inflammatory condition triggered by inflammatory cytokines, is the leading cause of most myocardial infarctions and many strokes, leading to high morbidity and mortality (73). Therefore, effective therapeutic strategies targeting ICAM-1 and VCAM-1 can be essential in these diseases. Here, we found that IL-32A94V mutant attenuated monocyte-endothelial adhesion, a critical early stage in atherosclerosis, by reducing the expression of ICAM-1 and VCAM-1. These results provide a new perspective on the previously known roles of IL-32 in vascular diseases. IL-32A94V binds to integrins and downregulates the phosphorylation of TNF- $\alpha$ -induced FAK, decreases the phosphorylation of intracellular signaling molecules, such as AKT, JNK, and I $\kappa$ B, and suppresses the nuclear translocation of AP-1 (c-Jun/c-Fos), and NF- $\kappa$ B (p65/p50). Taken together, IL-32A94V attenuated monocyte-endothelial adhesion by

suppressing the expression of ICAM-1 and VCAM-1, which are key factors in atherosclerosis, via integrin-mediated signaling in HUVECs (Figure 9). This evidence demonstrates the potential role of IL-32A94V in the treatment of chronic inflammatory diseases such as atherosclerosis. However, further studies on IL-32A94V are required using *in vivo* models. Moreover, the possibility of other unidentified cell surface receptors for IL-32 should be investigated. In addition, comparison studies of IL-32A94V with other isoforms should be performed under various conditions. These studies are important for understanding IL-32 and its mutant, as well as the overall function of IL-32.

## Data availability statement

The original contributions presented in the study are included in the article/supplementary materials, further inquiries can be directed to the corresponding author/s.

## Author contributions

J-YP and H-MP performed the experiments and wrote the main manuscript text. SK and K-BJ contributed to the analysis and interpretation of the data. C-ML reviewed and revised the manuscript. D-YY and JH supervised the experiments, contributed

to the interpreted the results, edited the manuscript. All authors contributed to the article and approved the final submitted version.

## Funding

This work was supported by the National Research Foundation of Korea (NRF) grant funded by the Korea government (MIST) (2021R1A2C 3014577, 2020R1A4A1018648).

## Acknowledgments

We would like to thank Editage ([www.editage.co.kr](http://www.editage.co.kr)) for English language editing (KOUNI\_5030).

## References

- Kim SH, Han SY, Azam T, Yoon DY, Dinarello CA. Interleukin-32: a cytokine and inducer of tnfnalpa. *Immunity* (2005) 22(1):131–42. doi: 10.1016/j.immuni.2004.12.003
- Joosten LA, Netea MG, Kim SH, Yoon DY, Oppers-Walgreen B, Radstake TR, et al. Il-32, a proinflammatory cytokine in rheumatoid arthritis. *Proc Natl Acad Sci U.S.A.* (2006) 103(9):3298–303. doi: 10.1073/pnas.0511233103
- Heinhuis B, Koenders MI, van de Loo FA, Netea MG, van den Berg WB, Joosten LA. Inflammation-dependent secretion and splicing of il-32{Gamma} in rheumatoid arthritis. *Proc Natl Acad Sci U.S.A.* (2011) 108(12):4962–7. doi: 10.1073/pnas.1016005108
- Netea MG, Azam T, Ferwerda G, Girardin SE, Walsh M, Park JS, et al. Il-32 synergizes with nucleotide oligomerization domain (Nod) 1 and Nod2 ligands for il-1beta and il-6 production through a caspase 1-dependent mechanism. *Proc Natl Acad Sci U.S.A.* (2005) 102(45):16309–14. doi: 10.1073/pnas.0508237102
- Shioya M, Nishida A, Yagi Y, Ogawa A, Tsujikawa T, Kim-Mitsuyama S, et al. Epithelial overexpression of interleukin-32alpha in inflammatory bowel disease. *Clin Exp Immunol* (2007) 149(3):480–6. doi: 10.1111/j.1365-2249.2007.03439.x
- Marcondes AM, Mhyre AJ, Stirewalt DL, Kim SH, Dinarello CA, Deeg HJ. Dysregulation of il-32 in myelodysplastic syndrome and chronic myelomonocytic leukemia modulates apoptosis and impairs nk function. *Proc Natl Acad Sci U.S.A.* (2008) 105(8):2865–70. doi: 10.1073/pnas.0712391105
- Sorrentino C, Di Carlo E. Expression of il-32 in human lung cancer is related to the histotype and metastatic phenotype. *Am J Respir Crit Care Med* (2009) 180(8):769–79. doi: 10.1164/rccm.200903-0400OC
- Kang YH, Park MY, Yoon DY, Han SR, Lee CI, Ji NY, et al. Dysregulation of overexpressed il-32alpha in hepatocellular carcinoma suppresses cell growth and induces apoptosis through inactivation of nf-kappab and bcl-2. *Cancer Lett* (2012) 318(2):226–33. doi: 10.1016/j.canlet.2011.12.023
- Na SJ, So SH, Lee KO, Choi YC. Elevated serum level of interleukin-32alpha in the patients with myasthenia gravis. *J Neurol* (2011) 258(10):1865–70. doi: 10.1007/s00415-011-6036-7
- Park JS, Choi SY, Lee JH, Lee M, Nam ES, Jeong AL, et al. Interleukin-32beta stimulates migration of mda-Mb-231 and mcf-7 cells Via the vegf-Stat3 signaling pathway. *Cell Oncol (Dordr)* (2013) 36(6):493–503. doi: 10.1007/s13402-013-0154-4
- Dos Santos JC, Barroso de Figueiredo AM, Teodoro Silva MV, Cirovic B, de Bree LCJ, Damen M, et al. Beta-Glucan-Induced trained immunity protects against leishmania braziliensis infection: a crucial role for il-32. *Cell Rep* (2019) 28(10):2659–72 e6. doi: 10.1016/j.celrep.2019.08.004
- Moreira Gabriel E, Wiche Salinas TR, Gosselin A, Larouche-Anctil E, Durand M, Landay AL, et al. Overt il-32 isoform expression at intestinal level during hiv-1 infection is negatively regulated by il-17a. *AIDS* (2021) 35(12):1881–94. doi: 10.1097/QAD.0000000000002972
- Goda C, Kanaji T, Kanaji S, Tanaka G, Arima K, Ohno S, et al. Involvement of il-32 in activation-induced cell death in T cells. *Int Immunol* (2006) 18(2):233–40. doi: 10.1093/intimm/dxh339
- Kang JW, Park YS, Lee DH, Kim MS, Bak Y, Ham SY, et al. Interaction network mapping among il-32 isoforms. *Biochimie* (2014) 101:248–51. doi: 10.1016/j.biochi.2014.01.013
- Shim S, Lee S, Hisham Y, Kim S, Nguyen TT, Taitt AS, et al. A paradoxical effect of interleukin-32 isoforms on cancer. *Front Immunol* (2022) 13:837590. doi: 10.3389/fimmu.2022.837590

## Conflict of interest

The authors declare that the research was conducted in the absence of any commercial or financial relationships that could be construed as a potential conflict of interest.

## Publisher's note

All claims expressed in this article are solely those of the authors and do not necessarily represent those of their affiliated organizations, or those of the publisher, the editors and the reviewers. Any product that may be evaluated in this article, or claim that may be made by its manufacturer, is not guaranteed or endorsed by the publisher.

- Pham TH, Bak Y, Kwon T, Kwon SB, Oh JW, Park JH, et al. Interleukin-32theta inhibits tumor-promoting effects of macrophage-secreted Ccl18 in breast cancer. *Cell Commun Signal* (2019) 17(1):53. doi: 10.1186/s12964-019-0374-y
- Bak Y, Kang JW, Kim MS, Park YS, Kwon T, Kim S, et al. Il-32theta downregulates Ccl5 expression through its interaction with pkcdelta and Stat3. *Cell Signal* (2014) 26(12):3007–15. doi: 10.1016/j.cellsig.2014.09.015
- Park HM, Park JY, Kim NY, Kim JJ, Pham TH, Hong JT, et al. Modulatory effects of point-mutated Il-32θ on tumor progression in triple-negative breast cancer cells. *Biofactors* (2023). BIOF-23-0115.
- Heinhuis B, Koenders MI, van den Berg WB, Netea MG, Dinarello CA, Joosten LA. Interleukin 32 (Il-32) contains a typical alpha-helix bundle structure that resembles focal adhesion targeting region of focal adhesion kinase-1. *J Biol Chem* (2012) 287(8):5733–43. doi: 10.1074/jbc.M111.288290
- Frank PG, Lisanti MP. Icam-1: role in inflammation and in the regulation of vascular permeability. *Am J Physiol Heart Circ Physiol* (2008) 295(3):H926–H7. doi: 10.1152/ajpheart.00779.2008
- Kong DH, Kim YK, Kim MR, Jang JH, Lee S. Emerging roles of vascular cell adhesion molecule-1 (Vcam-1) in immunological disorders and cancer. *Int J Mol Sci* (2018) 19(4):1057. doi: 10.3390/ijms19041057
- Yusuf-Makagiansar H, Anderson ME, Yakovleva TV, Murray JS, Siahaan TJ. Inhibition of lfa-1/Icam-1 and vla-4/Vcam-1 as a therapeutic approach to inflammation and autoimmune diseases. *Med Res Rev* (2002) 22(2):146–67. doi: 10.1002/med.10001
- Stanciu LA, Djukanovic R. The role of icam-1 on T-cells in the pathogenesis of asthma. *Eur Respir J* (1998) 11(4):949–57. doi: 10.1183/09031936.98.11040949
- Veale DJ, Maple C. Cell adhesion molecules in rheumatoid arthritis. *Drugs Aging* (1996) 9(2):87–92. doi: 10.2165/00002512-199609020-00003
- Troncoso MF, Ortiz-Quintero J, Garrido-Moreno V, Sanhueza-Olivares F, Guerrero-Moncayo A, Chiong M, et al. Vcam-1 as a predictor biomarker in cardiovascular disease. *Biochim Biophys Acta Mol Basis Dis* (2021) 1867(9):166170. doi: 10.1016/j.bbdis.2021.166170
- Azcutia V, Abu-Taha M, Romacho T, Vazquez-Bella M, Matesanz N, Luscinskias FW, et al. Inflammation determines the pro-adhesive properties of high extracellular d-glucose in human endothelial cells *in vitro* and rat microvessels *in vivo*. *PLoS One* (2010) 5(4):e10091. doi: 10.1371/journal.pone.00110091
- Wang Y, Cao J, Fan Y, Xie Y, Xu Z, Yin Z, et al. Artemisinin inhibits monocyte adhesion to huvecs through the nf-kappab and mapk pathways *in vitro*. *Int J Mol Med* (2016) 37(6):1567–75. doi: 10.3892/ijmm.2016.2579
- Vestweber D. How leukocytes cross the vascular endothelium. *Nat Rev Immunol* (2015) 15(11):692–704. doi: 10.1038/nri3908
- Lefer DJ, Granger DN. Monocyte rolling in early atherogenesis: vital role in lesion development. *Circ Res* (1999) 84(11):1353–5. doi: 10.1161/01.res.84.11.1353
- Lusis AJ. Atherosclerosis. *Nature* (2000) 407(6801):233–41. doi: 10.1038/35025203
- Tabas I. 2016 Russell Ross Memorial lecture in vascular biology: molecular-cellular mechanisms in the progression of atherosclerosis. *Arterioscler Thromb Vasc Biol* (2017) 37(2):183–9. doi: 10.1161/ATVBAHA.116.308036
- Ross R. Atherosclerosis is an inflammatory disease. *Am Heart J* (1999) 138(5 Pt 2):S419–20. doi: 10.1016/s0002-8703(99)70266-8

33. Frostegard J. Immunity, atherosclerosis and cardiovascular disease. *BMC Med* (2013) 11:117. doi: 10.1186/1741-7015-11-117
34. Greaves DR, Gordon S. Immunity, atherosclerosis and cardiovascular disease. *Trends Immunol* (2001) 22(4):180–1. doi: 10.1016/s1471-4906(00)01848-2
35. Maguire EM, Pearce SWA, Xiao Q. Foam cell formation: a new target for fighting atherosclerosis and cardiovascular disease. *Vascul Pharmacol* (2019) 112:54–71. doi: 10.1016/j.vph.2018.08.002
36. Heinhuis B, Popa CD, van Tits BL, Kim SH, Zeeuwen PL, van den Berg WB, et al. Towards a role of interleukin-32 in atherosclerosis. *Cytokine* (2013) 64(1):433–40. doi: 10.1016/j.cyto.2013.05.002
37. Nold-Petry CA, Nold MF, Zepp JA, Kim SH, Voelkel NF, Dinarello CA. IL-32-Dependent effects of IL-1 $\beta$  on endothelial cell functions. *Proc Natl Acad Sci U.S.A.* (2009) 106(10):3883–8. doi: 10.1073/pnas.0813334106
38. Kim KH, Shim JH, Seo EH, Cho MC, Kang JW, Kim SH, et al. Interleukin-32 monoclonal antibodies for immunohistochemistry, Western blotting, and Elisa. *J Immunol Methods* (2008) 333(1–2):38–50. doi: 10.1016/j.jim.2007.12.017
39. Yang J, Yan R, Roy A, Xu D, Poisson J, Zhang Y. The I-tasser suite: protein structure and function prediction. *Nat Methods* (2015) 12(1):7–8. doi: 10.1038/nmeth.3213
40. Yang J, Zhang Y. I-Tasser server: new development for protein structure and function predictions. *Nucleic Acids Res* (2015) 43(W1):W174–81. doi: 10.1093/nar/gkv342
41. Zheng W, Zhang C, Li Y, Pearce R, Bell EW, Zhang Y. Folding non-homologous proteins by coupling deep-learning contact maps with I-tasser assembly simulations. *Cell Rep Methods* (2021) 1(3):100014. doi: 10.1016/j.crmeth.2021.100014
42. Huang SY, Zou X. An iterative knowledge-based scoring function for protein-protein recognition. *Proteins* (2008) 72(2):557–79. doi: 10.1002/prot.21949
43. Huang SY, Zou X. A knowledge-based scoring function for protein-rna interactions derived from a statistical mechanics-based iterative method. *Nucleic Acids Res* (2014) 42(7):e55. doi: 10.1093/nar/gku077
44. Yan Y, Wen Z, Wang X, Huang SY. Addressing recent docking challenges: a hybrid strategy to integrate template-based and free protein-protein docking. *Proteins* (2017) 85(3):497–512. doi: 10.1002/prot.25234
45. Yan Y, Zhang D, Zhou P, Li B, Huang SY. Hdock: a web server for protein-protein and protein-DNA/Rna docking based on a hybrid strategy. *Nucleic Acids Res* (2017) 45(W1):W365–W73. doi: 10.1093/nar/gkx407
46. Yan Y, Tao H, He J, Huang SY. The hdock server for integrated protein-protein docking. *Nat Protoc* (2020) 15(5):1829–52. doi: 10.1038/s41596-020-0312-x
47. Livak KJ, Schmittgen TD. Analysis of relative gene expression data using real-time quantitative pcr and the 2 $^{-\Delta\Delta C_T}$  method. *Methods* (2001) 25(4):402–8. doi: 10.1006/meth.2001.1262
48. Bradford MM. A rapid and sensitive method for the quantitation of microgram quantities of protein utilizing the principle of protein-dye binding. *Anal Biochem* (1976) 72:248–54. doi: 10.1006/abio.1976.9999
49. Petersen EJ, Miyoshi T, Yuan Z, Hirohata S, Li JZ, Shi W, et al. Sirna silencing reveals role of vascular cell adhesion molecule-1 in vascular smooth muscle cell migration. *Atherosclerosis* (2008) 198(2):301–6. doi: 10.1016/j.atherosclerosis.2007.10.015
50. Ramer R, Bublitz K, Freimuth N, Merkord J, Rohde H, Hausteim M, et al. Cannabidiol inhibits lung cancer cell invasion and metastasis Via intercellular adhesion molecule-1. *FASEB J* (2012) 26(4):1535–48. doi: 10.1096/fj.11-198184
51. Schneider CA, Rasband WS, Eliceiri KW. Nih image to imagej: 25 years of image analysis. *Nat Methods* (2012) 9(7):671–5. doi: 10.1038/nmeth.2089
52. Yang CM, Luo SF, Hsieh HL, Chi PL, Lin CC, Wu CC, et al. Interleukin-1 $\beta$  induces icam-1 expression enhancing leukocyte adhesion in human rheumatoid arthritis synovial fibroblasts: involvement of erk, jnk, ap-1, and nf-kappab. *J Cell Physiol* (2010) 224(2):516–26. doi: 10.1002/jcp.22153
53. Kim KH, Park JK, Choi YW, Kim YH, Lee EN, Lee JR, et al. Hexane extract of aged black garlic reduces cell proliferation and attenuates the expression of icam-1 and Vcam-1 in tnf-Alpha-Activated human endometrial stromal cells. *Int J Mol Med* (2013) 32(1):67–78. doi: 10.3892/ijmm.2013.1362
54. Son DJ, Jung YY, Seo YS, Park H, Lee DH, Kim S, et al. Interleukin-32 $\alpha$  inhibits endothelial inflammation, vascular smooth muscle cell activation, and atherosclerosis by upregulating Timp3 and reek through suppressing mRNA-205 biogenesis. *Theranostics* (2017) 7(8):2186–203. doi: 10.7150/thno.18407
55. Lin X, Yang L, Wang G, Zi F, Yan H, Guo X, et al. Interleukin-32 $\alpha$  promotes the proliferation of multiple myeloma cells by inducing production of il-6 in bone marrow stromal cells. *Oncotarget* (2017) 8(54):92841–54. doi: 10.18632/oncotarget.21611
56. Kobayashi H, Huang J, Ye F, Shyr Y, Blackwell TS, Lin PC. Interleukin-32 $\beta$  propagates vascular inflammation and exacerbates sepsis in a mouse model. *PLoS One* (2010) 5(3):e9458. doi: 10.1371/journal.pone.0009458
57. Park MH, Yoon DY, Ban JO, Kim DH, Lee DH, Song S, et al. Decreased severity of activated T cells Via dendritic cell-derived Ccl5. *Biochem Biophys Res Commun* (2014) 450(1):30–5. doi: 10.1016/j.bbrc.2014.05.052
58. Kim MS, Kang JW, Jeon JS, Kim JK, Kim JW, Hong J, et al. IL-32 $\theta$  gene expression in acute myeloid leukemia suppresses tnf- $\alpha$  production. *Oncotarget* (2015) 6(38):40747–61. doi: 10.18632/oncotarget.5688
59. Bak Y, Kwon T, Bak IS, Hong J, Yu DY, Yoon DY. IL-32 $\theta$  inhibits stemness and epithelial-mesenchymal transition of cancer stem cells Via the Stat3 pathway in colon cancer. *Oncotarget* (2016) 7(6):7307–17. doi: 10.18632/oncotarget.7007
60. Shim S, Lee S, Hisham Y, Kim S, Nguyen TT, Taitt AS, et al. Comparison of the seven interleukin-32 isoforms' biological activities: il-32 $\theta$  possesses the most dominant biological activity. *Front Immunol* (2022) 13:837588. doi: 10.3389/fimmu.2022.837588
61. Hayman EG, Pierschbacher MD, Suzuki S, Ruoslahti E. Vitronectin—a major cell attachment-promoting protein in fetal bovine serum. *Exp Cell Res* (1985) 160(2):245–58. doi: 10.1016/0014-4827(85)90173-9
62. Takada Y, Takada YK, Fujita M. Crosstalk between insulin-like growth factor (Igf) receptor and integrins through direct integrin binding to Igf1. *Cytokine Growth Factor Rev* (2017) 34:67–72. doi: 10.1016/j.cytogfr.2017.01.003
63. Barczyk M, Carracedo S, Gullberg D. Integrins. *Cell Tissue Res* (2010) 339(1):269–80. doi: 10.1007/s00441-009-0834-6
64. Yoon H, Dehart JP, Murphy JM, Lim ST. Understanding the roles of fak in cancer: inhibitors, genetic models, and new insights. *J Histochem Cytochem* (2015) 63(2):114–28. doi: 10.1369/0022155414561498
65. Liu S, Xu SW, Kennedy L, Pala D, Chen Y, Eastwood M, et al. Fak is required for tgfbeta-induced jnk phosphorylation in fibroblasts: implications for acquisition of a matrix-remodeling phenotype. *Mol Biol Cell* (2007) 18(6):2169–78. doi: 10.1091/mbc.e06-12-1121
66. Oudart JB, Doue M, Vautrin A, Brassart B, Sellier C, Dupont-Deshorgue A, et al. The anti-tumor Nc1 domain of collagen xix inhibits the fak/ Pi3k/Akt/Mtor signaling pathway through Alphavbeta3 integrin interaction. *Oncotarget* (2016) 7(2):1516–28. doi: 10.18632/oncotarget.6399
67. Pflugfelder SC, Stern M, Zhang S, Shojaei A. Lfa-1/ICAM-1 interaction as a therapeutic target in dry eye disease. *J Ocul Pharmacol Ther* (2017) 33(1):5–12. doi: 10.1089/jop.2016.0105
68. Kotteas EA, Boulas P, Gkiozos I, Tsagkoulis S, Tsoukalas G, Syrigos KN. The intercellular cell adhesion molecule-1 (Icam-1) in lung cancer: implications for disease progression and prognosis. *Anticancer Res* (2014) 34(9):4665–72.
69. Perkins TN, Oczypok EA, Milutinovic PS, Dutz RE, Oury TD. Rage-dependent vcam-1 expression in the lung endothelium mediates il-33-Induced allergic airway inflammation. *Allergy* (2019) 74(1):89–99. doi: 10.1111/all.13500
70. Gao S, Yu L, Zhang J, Li X, Zhou J, Zeng P, et al. Expression and clinical significance of vcam-1, il-6, and il-17a in patients with allergic rhinitis. *Ann Palliat Med* (2021) 10(4):4516–22. doi: 10.21037/apm-21-546
71. Libby P, Buring JE, Badimon L, Hansson GK, Deanfield J, Bittencourt MS, et al. Atherosclerosis. *Nat Rev Dis Primers* (2019) 5(1):56. doi: 10.1038/s41572-019-0106-z